

The configural shape illusion

Karen B. Schloss

Department of Cognitive, Linguistic,
and Psychological Sciences, Brown University,
Providence, RI, USA



Francesca C. Fortenbaugh

Psychology Department, University of California,
Berkeley, CA, USA



Stephen E. Palmer

Psychology Department, University of California,
Berkeley, CA, USA



A new illusion, called the configural shape illusion (CSI), is described in which the apparent shape of an object (the “target”) is systematically distorted by the presence of an adjacent shape (the “inducer”) that is distinct from, but perceptually grouped with, the target. The target is selectively elongated in a direction consistent with the extension of the larger configuration that includes both target and inducer. Experiments 1 and 2 show that the CSI magnitude varies systematically with factors known to influence grouping strength between configural elements, including proximity, good continuation, positional alignment, lightness similarity, hue similarity, and common fate. Experiments 3 through 5 examine the influence of relative inducer size and target size on illusion magnitude. We suggest that the CSI is caused by edge assimilation modulated by similarity between the target and inducer arising from population coding of edge positions. This assimilation account fits well with previous explanations of one-dimensional illusions of linear extent (e.g., the Müller-Lyer and Baldwin illusions), which are extended to account for the present two-dimensional illusion of shape.

Introduction

People seldom perceive an object in isolation. Objects are almost always seen in spatial proximity to other objects, whose shapes, sizes, and colors may influence the perception of corresponding properties of the target object. In this article, we report a new spatial illusion called the configural shape illusion (CSI), in which the apparent shape of a target object is systematically distorted by adjacent shapes that are distinct from, but perceptually grouped with, that target. Figure 1 shows an example of the CSI. The

black rectangle on the left (the “target” rectangle; Figure 1A) is physically identical to the black rectangle on the right (the “comparison” rectangle; Figure 1B). However, the target appears to be taller than the comparison rectangle due to the presence of a gray semicircle (the “inducer”) that is attached to the target’s upper edge. We call this phenomenon the CSI because the target’s shape appears to be most distorted when, as we will show, the target and inducer are strongly integrated into a single, coherent configuration.

We first noticed the CSI while viewing displays of the occlusion illusion (Kanizsa, 1979; Palmer, Brooks, & Lai, 2007; Palmer & Schloss, 2009). The stimulus is the same physical configuration (see Figure 1A, C), but in the occlusion illusion the semicircle functions as the target and the rectangle as the inducer. The occlusion illusion occurs when the presence of the partly occluding rectangle makes the partly occluded semicircle (Figure 1A) appear taller (and thus bigger) than a nearby isolated semicircle that is physically identical (Figure 1C). The visual system seems to fill in a thin strip of the partly occluded object (here, the semicircle) along the occluding border due to mechanisms involving the perception of relative depth and partly occluded objects (Palmer et al., 2007; Palmer & Schloss, 2009). Despite the similarity in the displays that produce these two illusions, they are unlikely to have the same cause. The occlusion illusion requires the target to appear partly hidden from view (Palmer et al., 2007), yet the target rectangle in the CSI appears to be fully visible (Figure 1A). We return to the dissociation between the occlusion illusion and the CSI in Experiment 1.

The aim of the experiments presented in this article was to determine what factors modulate the CSI and

Citation: Schloss, K. B., Fortenbaugh, F. C., & Palmer, S. E. (2014). The configural shape illusion. *Journal of Vision*, 14(8):23, 1–18, <http://www.journalofvision.org/content/14/8/23>, doi:10.1167/14.8.23.

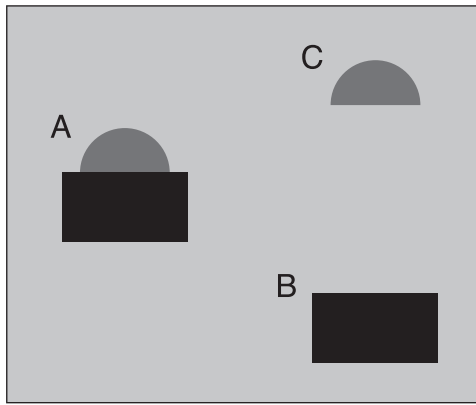


Figure 1. Comparison of the CSI and the occlusion illusion. In the CSI, the black rectangle in the configuration (the “target”; A) appears taller than a physically identical comparison rectangle (B). In the occlusion illusion, the semicircle in the configuration (A) appears taller than a physically identical semicircle (C).

what mechanisms might underlie it. Our initial informal investigations led us to suspect that the illusion is systematically influenced by perceptual grouping (see Palmer, 1999): The more strongly the target and inducer were grouped together, the larger the CSI appeared to be. Experiments 1 and 2 tested this hypothesis by measuring the strength of the CSI as the degree of target–inducer grouping varied using well-known factors such as proximity, good continuation, lightness similarity, and common fate (Wagemans et al., 2012; Wertheimer, 1923, 2012). We found that the illusion was indeed larger when there was stronger evidence that the target and inducer were part of a single configuration. Whether grouping per se or mere feature-based similarity is the better way to understand the phenomenon is an issue we address later.

The results of Experiments 3 through 5, however, suggest that the main underlying mechanism of the CSI involves assimilation errors in edge localization, which are then modulated by the same similarity factors that influence grouping strength. In the General discussion we argue that this account unifies several different kinds of illusions, including those of one-dimensional extent (e.g., the Müller-Lyer and Baldwin illusions), two-dimensional size (e.g., the Ebbinghaus and Delboeuf illusions), and two-dimensional shape (the CSI and shrinkage illusion).

Experiment 1

The primary purpose of Experiment 1 was to explore the hypothesis that CSI magnitude is influenced by the strength of grouping between the inducer and target. We measured the CSI using the method of adjustment.

Participants viewed displays similar to Figure 1A and B and were asked to adjust the height and width of the comparison rectangle (Figure 1B) so that it exactly matched the target rectangle in the configuration (Figure 1A). We varied four factors known to affect grouping strength robustly (proximity, good continuation, alignment, and lightness similarity), all of which are expected to increase the magnitude of the illusion. An additional condition designed to assess the role of depth and occlusion was included to dissociate the CSI from the superficially related occlusion illusion. We also examined the generality of the CSI by using two different inducer shapes with the same length and width: either half of a circle (as in Figure 1A) or half of a square.

Methods

Participants

Twenty participants with normal or corrected-to-normal vision volunteered for payment or partial course credit. All participants in this and all subsequent experiments gave informed consent, and the University of California Berkeley Committee for the Protection of Human Subjects approved the experimental protocol.

Design, displays, and procedure

For this and all subsequent experiments, participants sat approximately 60 cm from a 20-in. iMac computer monitor (1680 × 1050 pixel resolution; 48.5 cm wide × 46.9 cm tall; 60 Hz refresh rate; Apple Inc., Cupertino, CA). The test items were generated and displayed using Presentation (www.neurobs.com). The experimental displays consisted of the target rectangle alone or together with an inducer shape in the upper left of the display and the adjustable comparison rectangle in the lower right (Figure 1A, B). The target and comparison rectangles were misaligned to prevent participants from using alignment cues to aid their adjustments. Participants adjusted the height and width of the comparison rectangle to match the target rectangle by pressing the following eight keys on the keyboard, with separate keys designated for large (5 pixel) and small (1 pixel) adjustments: Q (large adjustment narrower), A (small adjustment narrower), W (large adjustment shorter), S (small adjustment shorter), P (large adjustment wider), L (small adjustment wider), O (large adjustment taller), and K (small adjustment taller).

The black (0.3 cd/m²) target rectangle was always 202 pixels wide × 144 pixels high on a medium-gray (50 cd/m²) background. The target was 12.0% of the

monitor width and 13.7% of the monitor height.¹ The following inducer conditions were tested.

No-inducer control: The target rectangle was presented without an inducer to provide a baseline for the adjustment task. All other conditions were compared with it, as we describe in the Results and discussion section.

Standard: The inducer was a dark gray (7 cd/m^2) rectangle (144 pixels wide \times 72 pixels high) or semicircle (144 pixels in diameter). It was centered horizontally above the target rectangle with its bottom edge touching the target rectangle's top edge. The inducer had these same parameters for all conditions unless otherwise specified.

Depth: We tested whether relative depth or occlusion influence the CSI by examining configurations in which a square (144 pixels wide \times 144 pixels high) or circular (144 pixels in diameter) inducer appeared in front of and partly occluded the target (see Figure 2A). We compared these conditions with the Standard configuration in which the inducer appeared behind the target.

Interior position: The inducer was centered inside rather than above the target (Figure 2B) to determine whether the illusion would be eliminated, or possibly even reverse, when the inducer was on the opposite side of the target's upper edge.

Lightness: Three inducer lightnesses—white (249 cd/m^2), the Standard dark gray (7 cd/m^2), and a darker gray (2 cd/m^2)—were tested to measure the effects of target–inducer lightness similarity (Figure 2C).

Connectedness and proximity: The bottom of the inducer was displaced upward by 0 (Standard), 10, or 100 pixels from the target's top edge to measure the effects of target–inducer connectedness and proximity (Figure 2D).

Width and continuation: Five inducer widths—28, 86, 144 (Standard), 202 (same as target), and 260 pixels—were tested to measure the effects of target–inducer width similarity and good continuation (Figure 2E).

Lateral position: The inducer was shifted laterally 75 pixels such that one edge extended 46 pixels beyond the target edge to measure the effects of target–inducer alignment (Figure 2F). The direction of lateral shift (left or right) was counterbalanced within participants.

Height: Three inducer heights—14, 72 (Standard), or 130 pixels—were tested to measure the effects of inducer height (Figure 2G).

Each of the 15 conditions described above was presented with both the rectangular and circular or semicircular inducers and was shown twice in the 60-trial experiment: once when the adjustable comparison rectangle was initially smaller (137 pixels wide \times 87 pixels high) than the true size of the target and once when it was initially larger (227 pixels wide \times 177 pixels high). All conditions were tested within subjects.

Results and discussion

We corrected for any biases in the basic experimental matching task by first subtracting the height and width values for the no-inducer control condition from the values for each experimental condition for each participant individually. That is, we calculated the magnitude of the illusion for each experimental display as the height and width (in pixels) of the adjustable rectangle matched to the target, minus the height and width of the adjustable rectangle from the matched, corresponding no-inducer control (i.e., a single rectangle with no inducing shapes in the same initial starting size condition, smaller or larger than the target). We then calculated the percentage of the adjustment difference relative to the true target size by dividing the difference by the length of the constant dimension (202 for width or 144 for height) and then multiplying by 100. A positive difference score in a particular dimension (e.g., height) indicates that participants perceived the target as larger in that experimental condition than in the no-inducer control condition.

The illusion magnitude, averaged over participants, is shown in Figure 2. These data are also averaged over the initial size of the adjustable rectangle and inducer shape (rectangles versus semicircles) because a repeated-measures analysis of variance (ANOVA) (inducer condition \times initial size \times inducer shape) revealed no main effects of initial size or inducer shape ($F_s < 1$) and no interactions between them and inducer condition (all $p > 0.05$). Based on our hypothesis that grouping between the target and inducer would bias the perception of target extent toward the corresponding dimension of the inducer, we predicted that the perceived height of the target would be significantly greater for all conditions except the Inside condition, for which we expected the opposite effect. Given these predictions, we did not correct for multiple comparisons on the height dimensions. The results are consistent with these predictions, as indicated by the asterisks over the bars in Figure 2, based on planned within-subjects t -tests against zero (see Table 1). We did not expect effects in the width dimension, so we applied the Bonferroni correction to account for the 14 t -tests against zero (adjusted alpha = 0.0036). None of the differences were significant after applying this correction. We also predicted that the illusion magnitude in the height dimension would be modulated by the degree of grouping between the target and the inducer according to classic grouping principles (Wagemans et al., 2012; Wertheimer, 1923, 2012). Note that there are 20, rather than 14, pairs of bars in Figure 2 because the Standard configuration is represented within each of the six subfigures (Figure 2A–G) to facilitate direct visual comparisons with the other configurations. The Standard configuration is denoted

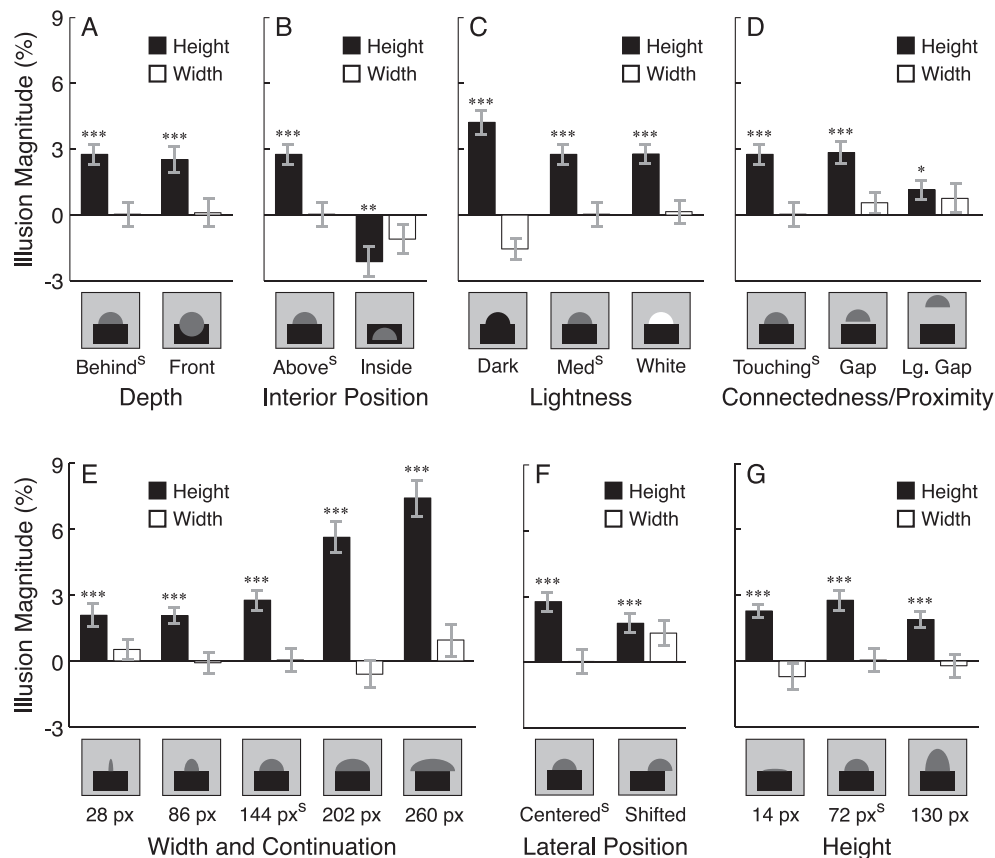


Figure 2. The average CSI magnitude for the height (black bars) and width (white bars) of the target for differences in inducer depth (A), interior position (B), lightness (C), connectedness and proximity (D), width and continuation (E), lateral position (F), and height (G). The same Standard configuration is present in each subplot, marked by the superscript “s,” but with different names in different subplots to indicate the relevant feature for that subplot. Asterisks indicate significant differences from zero (* $p < 0.05$, ** $p < 0.01$, *** $p < 0.001$; see Table 1). The error bars represent the standard errors of the means.

by a superscript “s” for the conditions labeled along the x-axes.

For the Standard configuration (Figure 2A, Table 1) there is a clear elongation of about 3% in the perceived height of the target, but no effect on its perceived width. This asymmetry indicates that the CSI is primarily a shape illusion due to the selective influence of the inducer’s extent on the corresponding target dimension. There were also no reliable effects on the target’s perceived width in the other conditions (Table 1).

First, we consider possible effects of occlusion to determine how closely the CSI might be related to its superficially similar cousin, the occlusion illusion (Kanizsa, 1979; Palmer et al., 2007; Palmer & Schloss, 2009). The occlusion illusion requires T-junctions (real or illusory) that specify that the occlusion illusion target (the gray semicircle in Figure 1A) is behind the occlusion illusion inducer (the black rectangle in Figure 1A). Even when stereoscopic depth cues specify that the target is in front of the occluder, monocular T-junctions are sufficient for the illusion to persist (Palmer & Schloss, 2009). However, when T-junctions

specify that the target is in front of the inducer, the illusion diminishes.

We tested for effects of occlusion by comparing the Standard configuration in which T-junctions specify that the CSI target (the black rectangle) occludes the CSI inducer (the gray semicircle or rectangle) with the Depth-reversed configuration in which T-junctions specify that the inducer occludes the target (the Front condition in Figure 2A). We compared the illusion magnitude in the height dimension for these two conditions using within-subjects difference-score t -tests. There was no difference between these conditions (all $t < 1$), indicating that depth ordering as specified by T-junctions does not influence CSI magnitude. The equivalent CSI magnitude in these two occlusion conditions thus implies that the CSI and the occlusion illusion arise from different underlying processes.

When the inducer is inside the target (Figure 2B), an opposite illusion occurs. The target appears significantly shorter in the Inside condition than in the Above (Standard) condition, as indicated by a within-subjects difference-score t -test, $t(19) = 7.28$, $p < 0.001$. As noted

Condition	Height <i>t</i>	Width <i>t</i>
Standard	6.19***	<1
Front	4.25***	<1
Inside	3.15**	1.65
Dark	7.89***	3.28
White	6.41***	<1
Gap	5.85***	1.16
Large gap	2.61*	1.15
Width (28 pixels)	3.99***	1.1
Width (86 pixels)	5.51***	<1
Width (202 pixels)	7.99***	<1
Width (260 pixels)	9.01***	1.3
Shifted	4.05***	2.32
Height (14 pixels)	7.17***	1.24
Height (130 pixels)	5.20***	<1

Table 1. Results of *t*-tests ($df = 19$) comparing the illusion magnitude with zero for each of the displays in Figure 2 (* $p < 0.05$, ** $p < 0.01$, *** $p < 0.001$). The *t*-tests in the height dimension were not corrected for multiple comparisons because the illusion was expected in all conditions. There was no expected illusion for the width dimension so the Bonferroni correction was applied for 14 comparisons. None of the resulting *t*-tests in the width dimension revealed significant differences from zero.

in Table 1, the target in the Inside condition also differed from zero. This shortening effect of the interior inducer is likely attributable to the same mechanisms as those underlying the CSI but working in the opposite direction. We return to this issue in the General discussion.

Next, we address our hypothesis that the CSI is modulated by the grouping strength between the target and inducer. By *grouping strength* we mean the amount of evidence from well-known grouping factors that the target and inducer are part of a single object or configuration, as opposed to being separate perceptual elements.

Figure 1C shows the effects of lightness similarity. A repeated-measures ANOVA comparing the three inducer lightness levels revealed a main effect, $F(2, 38) = 9.31$, $p < 0.001$. Subsequent difference-score *t*-tests revealed that the target appeared reliably taller when the inducer was dark gray (and thus more similar to the black target) than when it was the Standard medium gray or white, $t(19) = 3.37, 4.42$ and $p < 0.01, 0.001$, respectively. There was no difference in illusion magnitude between the medium gray and white inducers ($t < 1$), however, suggesting that lightness similarity increases the CSI only when target and inducer lightnesses are highly similar and that its impact diminishes once the target and inducer are sufficiently different.

Grouping by connectedness (Palmer & Rock, 1994) and proximity predicts that the CSI should diminish as connectedness is eliminated and the distance between

target and inducer increases. A repeated-measures ANOVA comparing the three gap conditions showed that there was a significant effect of gap size, $F(2, 38) = 10.68$, $p < 0.001$ (see Figure 2D). Subsequent planned comparisons via within-subjects difference-score *t*-tests further indicated that the Small-gap and the No-gap (Standard) conditions produced stronger height illusions than did the Large-gap condition, $t(19) = 4.11, 3.85$, $p < 0.01$. The Small-gap and No-gap conditions did not differ from each other ($t < 1$), apparently indicating that target–inducer connectedness is not critical for the illusion provided that the target and inducer are strongly grouped into a single configuration by proximity. The fact that the illusion persists across a clearly perceptible gap constitutes further evidence that occlusion is not likely to be a relevant factor in the CSI. However, it may be compatible with accounts based on edges falling within overlapping receptive fields—an issue to which we return in the General discussion.

We next tested whether target–inducer good continuation and similarity in width modulated the illusion (Figure 2E). A repeated-measures ANOVA on the five inducer widths revealed that the target’s perceived height varied with inducer width, $F(4, 76) = 24.66$, $p < 0.001$. Subsequent comparisons revealed no difference in illusion magnitude (2%–3%) among the three configurations in which the inducer was narrower than the target, $F(2, 38) = 1.53$, $p > 0.05$. However, when the widths of the inducer and target were the same and their edges were aligned, the illusion was reliably greater (6%) than the average of the three narrower conditions, $F(1, 19) = 18.64$, $p < 0.001$, consistent with grouping by similarity and good continuation. The fact that the illusion was marginally greater for the widest inducer than for the aligned inducer (10 pixels, or 7%), $F(1, 19) = 4.20$, $p = 0.06$, may be at least partly due to contributions of the occlusion illusion in this configuration because the T-junctions along the shared edge strongly imply that the target extends behind the inducer.

In a similar vein, aligning the inducer with the center of the target produced a larger height illusion than did shifting the inducer right or left (Figure 2F), as indicated by a main effect of lateral position in a repeated-measures ANOVA of the two inducer placements, $F(1, 19) = 6.28$, $p < 0.05$ (Figure 2E). (For this analysis and in Figure 2F, leftward and rightward shifts were combined because shift direction had no effect on illusion magnitude, $t < 1$). Lateral displacements also produced a slight width illusion, although it did not reach significance after correcting for multiple comparisons (see Table 1). Still, we note that this marginal width effect may be due to the same mechanisms as the basic CSI, given that the inducer has boundaries that extend beyond the edges of the target in the relevant

dimension, just as the basic CSI does in the orthogonal direction.

Finally, Figure 2G suggests that increasing the inducer's height produces a nonmonotonic effect on the target's perceived height. Although a repeated-measures ANOVA of the three inducer heights indicated that the effect of inducer height was not significant in these data, $F(2, 38) = 1.59$, $p = 0.22$, this inverted U-shaped function turns out to be robust when measured more extensively in Experiments 3 through 5. Indeed, the shape of this function provides an important clue about the edge mislocalization mechanism we propose to underlie the CSI in the General discussion.

Experiment 2

Experiment 2 had several purposes. First, it attempted to generalize the CSI to different shapes by using oval targets as well as rectangular ones. Second, it investigated directional and positional effects by placing the inducer either along the top of the target (as in Experiment 1) or along its right side. Third, it employed a different procedure for measuring the magnitude of the illusion that did not involve matching the target to a separate standard figure. Rather, we asked participants to adjust the target object itself to be perfectly square or perfectly circular in the presence versus absence of an inducer. The results for the configural conditions were corrected for the well-known horizontal-vertical illusion that true squares and true circles appear somewhat taller than they are wide (Avery & Day, 1969; Finger & Spelt, 1947) by comparing them with corresponding control conditions in which no inducer was present. Fourth, because the target in Experiment 1 was always darker than the inducer and the inducer was almost always darker than the background, Experiment 2 examined all possible differences in contrast polarity among the target, inducer, and background. Fifth, it measured the effects of two further variables that should influence the magnitude of the illusion if grouping strength is important: hue similarity and common fate.

Methods

Participants

Fourteen participants with normal or corrected-to-normal vision and normal color vision (as tested by the Dvorine pseudoisochromatic plates) participated in this experiment for payment or partial course credit.

Design, displays, and procedure

The displays consisted of either a target-inducer configuration or the target-alone control, all of which were presented on the same monitor and under the same viewing conditions as in Experiment 1. The target was either rectangular or elliptical, and participants were asked to adjust the target's shape to form a perfect square or perfect circle, respectively. The inducer was adjacent to either the top or right edge of the target. When the inducer was above the target, the target's bottom edge was adjustable by sliding the mouse up and down. When the inducer was to the right of the target, the target's left edge was adjustable by sliding the mouse left and right. When participants were satisfied with their adjustments, they clicked the mouse to record their response.

As in Experiment 1, the inducer shape was either a circle (144 pixels in diameter) or a square (144×144 pixels) that was partly occluded by the rectangular or elliptical target. The inducers were placed with their centers at the middle of the top or right edge of the target. Thus, for square targets, the visible portion of the partly occluded circular inducer was a semicircle and that of the partly occluded square inducer was a rectangle whose aspect ratio was 2:1. For circular targets, the partly occluded circular inducer was a crescent and the partly occluded square inducer was a rectangle-like quadrilateral with one concave edge (see Figure 3). For simplicity we still refer to these inducers as semicircles and rectangles, respectively. At the start of each trial, the target was either taller or wider than a perfect square or circle. The nonadjustable dimension was always 200 pixels, and the initial value of the adjustable dimension was either 150 pixels or 250 pixels. The inducer and target configurations were as follows.

Lightness contrast: Six lightness contrast combinations were tested, including all possible assignments of black (0.3 cd/m^2), gray (50 cd/m^2), and white (249 cd/m^2) to the background, target, and inducer such that no two regions had the same luminance. There were 96 target-inducer configurations, including 2 target shapes (square or circle) \times 2 inducer shapes (rectangle or semicircle) \times 2 target initial sizes (smaller or larger) \times 2 adjustable dimensions (height or width) \times 6 lightness contrast combinations, plus corresponding no-inducer control conditions.

Hue contrast: Four hue contrast combinations were tested in which the target and inducer were assigned all possible isoluminant pairs of red (26 cd/m^2) and green (luminance determined individually by heterochromatic flicker photometry; Wagner & Boynton, 1972). There were 64 conditions, including 2 target shapes (square or circle) \times 2 inducer shapes (rectangle or semicircle) \times 2 target initial sizes (smaller or larger) \times 2 adjustable

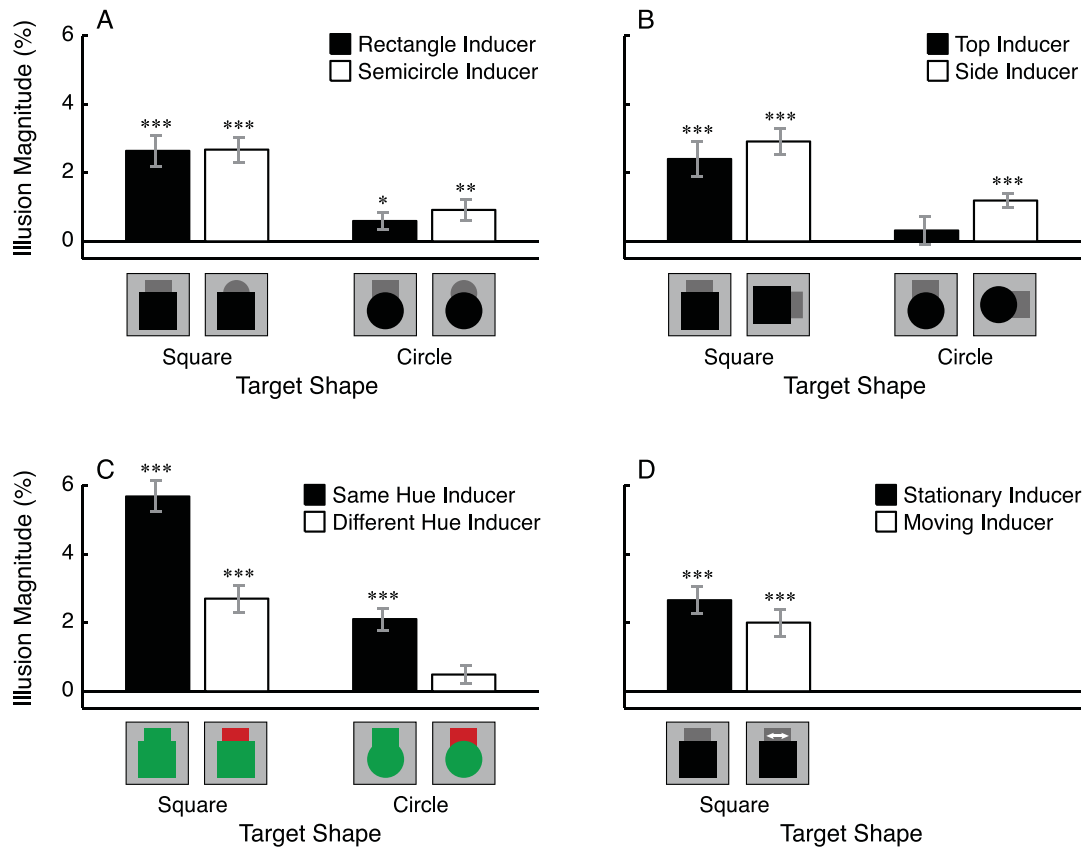


Figure 3. Average CSI magnitude (in percentage of target extent relative to the nonadjusted dimension) as a function of target shape (square or circle) and (A) inducer shape (rectangle or semicircle) for the stationary, lightness similarity configurations averaged over orientations, (B) inducer position and orientation for the stationary, lightness similarity configurations averaged over inducer shapes, (C) hue similarity (same or different) averaged over inducer shapes, and (D) inducer motion (for square targets only) averaged over inducer shapes. The error bars represent the standard errors of the means. Asterisks indicate significant differences from zero ($*p < 0.05$, $**p < 0.01$, $***p < 0.001$).

dimensions (height or width) \times 4 hue combinations, plus corresponding no-inducer control conditions.

Common fate: The inducer moved throughout the trial over a range of 40 pixels (± 20 pixels from its center-aligned position) at a speed of 1 pixel/frame relative to the stationary target. Only the square target was tested because the visible portion of the inducer's shape was invariant during its motion, whereas the inducer would have changed shape as it moved behind the circular target (i.e., the inducer would have "peeked out" beyond the left and right of the circular target due to its curvature). There were 48 conditions, including 2 inducer shapes (rectangle or semicircle) \times 2 initial sizes (smaller or larger) \times 2 adjustable dimensions (height or width) \times 6 luminance combinations (see lightness contrast conditions above). These conditions were compared with the corresponding stationary conditions (see lightness contrast above) to measure effects of common fate.

Results and discussion

We first measured the horizontal-vertical illusion in the no-inducer control conditions by subtracting the adjusted dimensional extent required to make a perfect square or perfect circle (200 pixels) from all responses. We then calculated the percentage of the adjustment difference relative to a perfect square or circle by dividing the difference by 200 (the length of the constant dimension, which would produce a geometrically perfect circle or square) and then multiplying by 100. To test for the statistical reliability of horizontal-vertical illusion effects, we conducted a four-way repeated-measures ANOVA: 2 target shapes (square or circle) \times 2 adjustment dimensions (height or width) \times 8 color combinations (six gray scale and two chromatic conditions; see Methods) \times 2 initial sizes (shorter or longer). Consistent with the classic horizontal-vertical illusion, there was a main effect of adjustable dimension, $F(1, 13) = 52.61$, $p < 0.001$: The vertical dimension was adjusted to be 4% shorter and the horizontal dimension

was adjusted to be 3% wider to compensate for the target appearing vertically elongated. The effect of adjustment dimension interacted with target shape, $F(1, 13) = 11.43$, $p < 0.01$, because the illusion was more pronounced for the square target (vertical: -6% ; horizontal: $+4\%$) than for the circle target (vertical: -2% ; horizontal: $+2\%$). This difference probably occurred because the only cue to a true square is aspect ratio, whereas true circles have the additional cue of constant curvature, which may be less sensitive to differences in orientation. These factors did not further interact with initial size or color, however ($F_s < 1$).

In calculating the CSI magnitude for each participant, we first subtracted the horizontal–vertical illusion from the CSI data by calculating the length of the adjusted target minus the length of the target in the no-inducer control condition that was matched for color, adjustable dimension (height or width), and initial size. In this difference score, the effects due to the horizontal–vertical illusion are removed so that the remaining illusion is due entirely to the CSI. To express the remaining CSI effect as a percentage, we then divided this difference score by the length required to make a perfect square or circle (i.e., 200 pixels—the length of the nonadjustable dimension) and multiplied by 100. The illusion is positive when the inducer causes the target to be seen as more extended in the measured dimension, which it did for all conditions (see Figure 3). Note that the present experimental procedure does not allow measurement of illusions in the orthogonal dimension.

We analyzed the overall effects of target shape (square or circle), inducer shape (rectangle or semicircle), configuration orientation (vertical or horizontal), achromatic contrast conditions (all six possible assignments of black, white, and gray to the background, target, and inducer), and initial size (larger or smaller) within a five-way repeated-measures ANOVA. As in Experiment 1 there was no main effect of initial size, $F(1, 13) = 2.51$, $p > 0.05$, and it did not interact with any of the other factors (all $p > 0.05$). There was also no effect of inducer shape (semicircle vs. rectangle), $F(1, 13) = 1.18$, $p > 0.05$, and it did not interact with target shape ($F < 1$). The lack of this interaction indicates that shape similarity between the inducer and target does not influence the magnitude of the illusion, at least within this range of shapes.

Figure 3A shows the effects of target shape (square vs. circle) on CSI magnitude averaged over participants, initial size, inducer location, and lightness. Both inducers produced reliable shape illusions (Table 2), but the illusion was substantially larger when participants adjusted the rectangle to make a perfect square than when they adjusted the oval to make a perfect circle, $t(13) = 3.92$, $p < 0.01$. This effect is in addition to the difference in the basic horizontal–vertical illusion

for squares versus circles (see above) because subtracting the no-inducer control data eliminated any horizontal–vertical illusion effects. The target shape effect may still be due to constant curvature in circles, but here it produces a reduction in the influence of the inducer on the circular targets.

We next compared configurations in which the inducer was above versus to the right of the target to confirm that the CSI is an illusion of extent in the direction that is orthogonal to the target and inducer's shared edge (i.e., a height illusion when the inducer is above and a width illusion when the inducer is on the side of the target; Figure 3B). These data are averaged over participants, initial size, inducer shape, and lightness. There were reliable illusions in both the vertical and horizontal dimensions (see Table 2), though not for the circle target when the inducer was above it. Further, there was no interaction between orientation and target shape ($t < 1$). The CSI is thus a shape illusion due to selective extension of the target shape in the direction of the farther boundary of the inducer. In the present data the illusion is roughly invariant over the position of the inducer relative to the target and the orientation of the dimension affected.

An overall repeated-measures ANOVA showed no effect of lightness contrast polarities among the target, inducer, and background, $F(5, 65) = 1.39$, $p > 0.05$, and this factor did not interact with target shape, inducer shape, or adjustable dimension ($F_s < 1$). Based on these results and the effects of lightness similarity in Experiment 1 (Figure 2C), we conclude that the illusion is larger when the target and inducer are highly similar in color (as in the Dark condition in Experiment 1), but once they reach some critical level of dissimilarity, the magnitude of the illusion is no longer affected by lightness similarity.

To examine effects of hue similarity we compared the same-hue displays (i.e., red target with red inducer and green target with green inducer) with the isoluminant different-hue conditions (i.e., red target with green inducer and green target with red inducer). These data, presented in Figure 3C, are averaged over participants, initial size, and inducer shapes. The data in the “Same hue inducer” conditions are also averaged over the red and green configurations, and the data in the “Different hue inducer” conditions are averaged over the target and inducer hue assignment (i.e., whether the target was red and inducer was green or vice versa). Compared with zero, reliable illusions were present for both the same hue and isoluminant different-hue conditions (see Table 2). A repeated-measures ANOVA [2 color relations (same or different) \times 2 target shapes (square or circle)] revealed that the CSI was substantially larger for the same-hue configurations than for the different-hue configurations, $F(1, 13) = 103.35$, $p < 0.001$. As before, it was also greater for the square

Target	Inducer	<i>t</i>
(A) Square	Rectangle	5.73***
(A) Square	Semicircle	7.30***
(A) Circle	Rectangle	2.28*
(A) Circle	Semicircle	3.08**
(B) Square	Top	4.72***
(B) Square	Side	7.54***
(B) Circle	Top	<1
(B) Circle	Side	5.74***
(C) Square	Same color	12.6***
(C) Square	Different color	5.28***
(C) Circle	Same color	8.32***
(C) Circle	Different color	1.89
(D) Square	Static	6.80***
(D) Square	Oscillating	5.10***

Table 2. Results of *t*-tests ($df = 13$) comparing the illusion magnitude with zero for each condition in Figure 4. The target column indicates the shape of the target, the letter in parentheses indicates the subplot of Figure 3 where the data are reported, and the inducer column indicates the inducer condition. The data are averaged over initial size for all conditions. In A the data are also averaged over inducer location and lightness; in B they are averaged over inducer shape and lightness; in C they are averaged over inducer shape, position, and color (within the same vs. different conditions); and in D they are averaged over inducer position and lightness.

target than the circle target, $F(1, 13) = 55.65$, $p < 0.001$. However, target shape interacted with hue similarity, $F(1, 13) = 14.95$, $p < 0.01$, in which the difference between the same-hue conditions and different-hue conditions was larger for the square target than the circle target. This effect is further evidence that square targets are more susceptible to inducer manipulations than are circle targets. Note that in same-hue displays there is zero contrast at the target–inducer border and that viewers must therefore extrapolate the visible target contours to judge the target’s aspect ratio. Nevertheless, it is unclear why the extrapolated border should be systematically perceived as displaced in the direction of the inducer except for whatever mechanisms underlie the CSI. This is an initial clue that those mechanisms may include edge mislocalization because it seems plausible that the visual system might be more strongly misled by the configural edge when extrapolating a zero-contrast target edge than when the target edge is clearly visible. The data also show that pure hue contrast (Figure 3C) produces just as strong an illusion as pure lightness contrast (Figure 3A) when averaging over all other conditions ($F < 1$).

Finally, we tested whether the CSI is modulated by common fate between the target and inducer. For this analysis, we averaged over inducer shape, initial size, adjustable dimensions, and lightness for the static and oscillating inducer conditions (Figure 3D). We collect-

ed data only for the square target for the oscillation condition (for reasons explained in the Methods section), which is why there is no circular target condition in Figure 3D. A within-subjects paired comparison of stationary versus moving inducers shows that the illusion was greater when the inducer was stationary than when it was oscillating, $t(13) = 3.03$, $p < 0.01$. This result supports the hypothesis that the CSI is larger when the target and inducer are more strongly grouped into a single coherent configuration by virtue of common fate (i.e., when both elements are stationary) than when grouping is weakened by differential motion. Although breaking common fate between the target and inducer decreased the illusion magnitude, the CSI was still highly reliable compared with zero (Table 2) when the inducer oscillated and the target did not.

Experiment 3

In Experiment 1 we found suggestive evidence for nonmonotonic variation in illusion strength as a function of the extent of the inducer (Figure 2G): The illusion was larger for the medium-height inducer than it was for the short and tall inducers. In Experiment 3 we tested a wider range of inducer lengths to determine at which inducer length the illusion is maximal and how illusion magnitude varies as a function of inducer length using the perfect square adjustment task of Experiment 2. We tested two inducer widths (narrower than and aligned with the target; see Figure 4) to measure how grouping by good continuation (aligned condition) might modulate inducer length effects. We also varied whether the inducer was positioned above, below, left of, or right of the target.

Methods

Participants

Eighteen participants with normal or corrected-to-normal vision volunteered for payment or partial course credit.

Design and displays

Trials types included the orthogonal combination of four factors: eight inducer lengths [0 (the no-inducer control), 10, 60, 110, 160, 210, 260, or 310 pixels], two inducer alignments [aligned with the target (200 pixels) or narrower (144 pixels)], four inducer locations (adjacent to the top, bottom, left, or right edge of the target), and two initial lengths for the adjustable dimension of the target [shorter (150 pixels) or longer

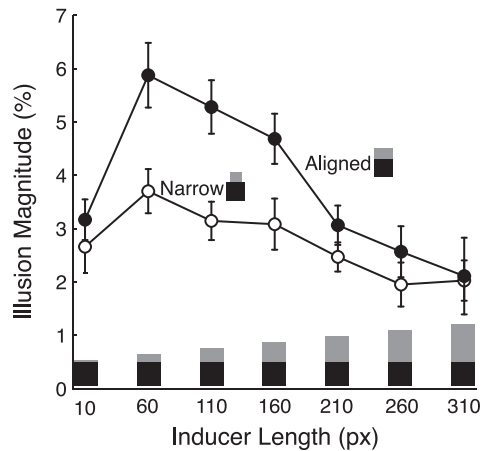


Figure 4. Average CSI magnitude (in percentage relative to the nonadjusted dimensional extent) as a function of inducer length for the aligned (closed symbols) and narrow (open symbols) inducers, averaged over the inducer orientations. Error bars represent the standard errors of the means.

(250 pixels) than the length that would produce a true square]. The shared edge between the target and inducer was always 100 pixels offset from the center of the screen, and the location of the opposite edge was adjustable. The target was always black (0.3 cd/m^2). The background was always gray (50 cd/m^2) and the inducer was always the standard gray (7 cd/m^2).

Procedure

The task was the same as that in Experiment 2 except that no circular targets were used. Participants were asked to adjust the variable dimension of the target to produce a perfect square by sliding the cursor to change its shape and clicking to record their response. Participants had control of the target's edge that was opposite the edge adjacent to the inducer (e.g., if the inducer was above the target, participants had control of the target's bottom edge; when it was to the left of the target, they had control of its right edge). There were 128 trials, with 500-ms intertrial intervals.

Results and discussion

As in Experiment 2, CSI magnitude was measured as the length of the adjusted target in each experimental condition minus the length of the target in the no-inducer control condition matched for adjustable edge (top, bottom, left, or right) and initial size. There was no stimulus difference between the control conditions corresponding to the “aligned” versus “narrow” inducer conditions because no inducer was present, so those trials were averaged. Illusion magnitude was coded so that it was positive when it occurred in the

expected direction, and the effects due to the horizontal-vertical illusion described above were removed by subtracting the control measurements from the other conditions so that the remaining illusion is due only to the CSI. As in Experiment 2, the difference scores were divided by the extent of the nonadjusted dimension (200 pixels) and multiplied by 100 to represent CSI magnitude as the percentage difference in target size.

To analyze the results we conducted a repeated-measures ANOVA with four orthogonal factors: two target widths (narrow or aligned), four inducer locations (top, bottom, left, or right), seven inducer heights (see Figure 4), and two initial sizes (larger or smaller than the target). The inducer position (top, bottom, left, or right) had no overall effect on the CSI magnitude, $F(3, 51) = 1.34$, $p > 0.05$, and did not interact with inducer length ($F < 1$). Inducer position did interact with alignment, $F(3, 51) = 5.64$, $p < 0.01$, in that alignment had a larger effect when the inducer was above or below the target than when it was left or right. The reason for this interaction is unclear.

The overall effects of inducer length (Figure 4) showed a robust quadratic within-subjects contrast, $F(1, 17) = 32.03$, $p < 0.001$. The illusion increased as inducer length increased from 10 to 60 pixels, $F(1, 17) = 30.84$, $p < 0.001$, and then decreased almost linearly from 60 to 310 pixels, $F(5, 85) = 15.42$, $p < 0.001$, but was still reliably greater than zero at 310 pixels, $F(1, 17) = 24.62$, $p < 0.001$. This is much stronger evidence of the nonmonotonic pattern found in Experiment 1 (Figure 2G). Also, as in Experiment 1 (Figure 2E), the illusion was greater when the inducer width was aligned with the target than when it was narrower, $F(1, 17) = 9.86$, $p < 0.01$. Alignment interacted with inducer length, however, in that the illusion was comparable for the two alignment conditions when the inducer was very small or very large but was reliably greater for the aligned inducers for the inducers with pixel length of 60 to 160, $F(6, 102) = 3.52$, $p < 0.01$. Good continuation thus appears to modulate the effects of inducer height.

Experiment 4

The results of Experiment 3 demonstrated that the CSI depends on the extent of the inducer but gave no indication of whether or how it might also be influenced by the extent of the target. Of particular interest is whether the illusion depends on metric properties that are absolute or relative to the configuration. Experiment 4 therefore examined the joint effects of varying both inducer and target extents in the edge-aligned configurations for which the illusion is maximal. We also included two versions of the configurations that differ in overall size to find out

whether the CSI is scale invariant. The larger set is comparable with those studied previously and the smaller set is scaled to half that size. In addition, we used the matching paradigm (as in Experiment 1) to generalize the findings of Experiment 3 over methods. Observers adjusted a stand-alone rectangle of variable length and width dimensions to equal the target rectangle in the illusion-inducing configuration.

Methods

Participants

There were two groups of participants: one tested on large configurations ($n = 12$) and one on small configurations ($n = 16$). All participants had normal or corrected-to-normal vision and volunteered for either payment or partial course credit.

Design, displays, and procedure

For the large-configuration participants, one dimension (height or width) of the target was always 200 pixels and the other dimension was 100, 200, or 300 pixels, producing six possible target shapes. The inducer, when present, was always adjacent to the 200-pixel side of the target (top or left edge). The inducer was aligned with the target such that one dimension was 200 pixels and the other dimension was 10, 40, 70, 100, 130, or 260 pixels. These, along with the no-inducer control conditions (0-pixel inducers), produced a total of 42 configurations. The target was always black (0.3 cd/m^2), the background was always gray (50 cd/m^2), and the inducer was always a darker gray (7 cd/m^2). Each configuration was presented six times: three in which the adjustable rectangle was initialized as a random size that was taller and narrower than the target and three in which it was initialized as a random size that was shorter and wider than the target. There were 252 trials.

The design was the same for the small-configuration participants, with the exception that all of the linear extents were half as large, and an additional inducer length was included. One dimension (height or width) of the target was always 100 pixels and the other dimension was 50, 100, or 150 pixels. The inducer, when present, was always adjacent to the 100-pixel side of the target (top or left edge). The inducer's dimension that was 100 pixels was aligned with the target, and the other dimension was 5, 20, 35, 50, 65, 130, or 260 pixels. These, along with the no-inducer control conditions (0-pixel inducers), produced a total of 48 configurations. With the six replications, there were 288 trials.

The center of the target was always located 250 pixels to the left of the vertical midline of the monitor

and centered on the horizontal midline. The adjustable rectangle that was used to match the target was located at the bottom right corner of the screen. The adjustable rectangle's bottom edge was fixed 450 pixels below the horizontal midline, and its right edge was fixed 700 pixels to the right of the midline. The top and left edges were adjustable by sliding the mouse so that participants perceived that they had control of its top left corner. Participants were instructed to match the adjustable rectangle exactly to the target by moving the mouse, and then to click to record their response. Displays remained on the screen until participants responded, and the next trial began 500 ms later.

Results and discussion

The goal of this experiment was to understand how the CSI scales with overall size, the extent of the target, and the extent of the inducer. We therefore began the analyses by representing the illusion magnitude in pixels rather than as the percentages of the total target extent as in the prior experiments (see Figure 5A, B). We measured CSI magnitude separately for the target's height and width, as in Experiment 1. The magnitude of the illusion for each experimental display is the height and width (in pixels) of the adjustable rectangle matched to the target, minus the height and width of the adjustable rectangle matched to the corresponding no-inducer control (i.e., a single rectangle with no inducing shapes in the same initial starting size condition). A positive difference score in a particular dimension (e.g., height) indicates that participants perceived the target as larger in that experimental condition than in the no-inducer control condition.

We conducted three-way target extent \times inducer extent \times inducer location repeated-measures ANOVAs for the dimension in which the illusion was expected (height for inducer-above configurations and width for inducer-left conditions). These ANOVAs were done separately for the large-configuration and small-configuration conditions, which was a between-subjects factor. There were three target extents for both the large- and small-configuration ANOVAs and two inducer locations, but there were six inducer extents for the large-configuration ANOVA and seven inducer extents for the small-configuration ANOVA.

The illusion magnitudes for the different size and extent conditions are shown in Figure 5 averaged over replications, initial sizes, inducer locations (top vs. side), and participants. The ANOVA for the large-configuration conditions (Figure 5A) revealed main effects of both target extent, $F(2, 22) = 44.03$, $p < 0.001$, and inducer extent, $F(5, 55) = 18.51$, $p < 0.001$. There was an interaction between target size and inducer location in which the illusion was greater when the inducer was on

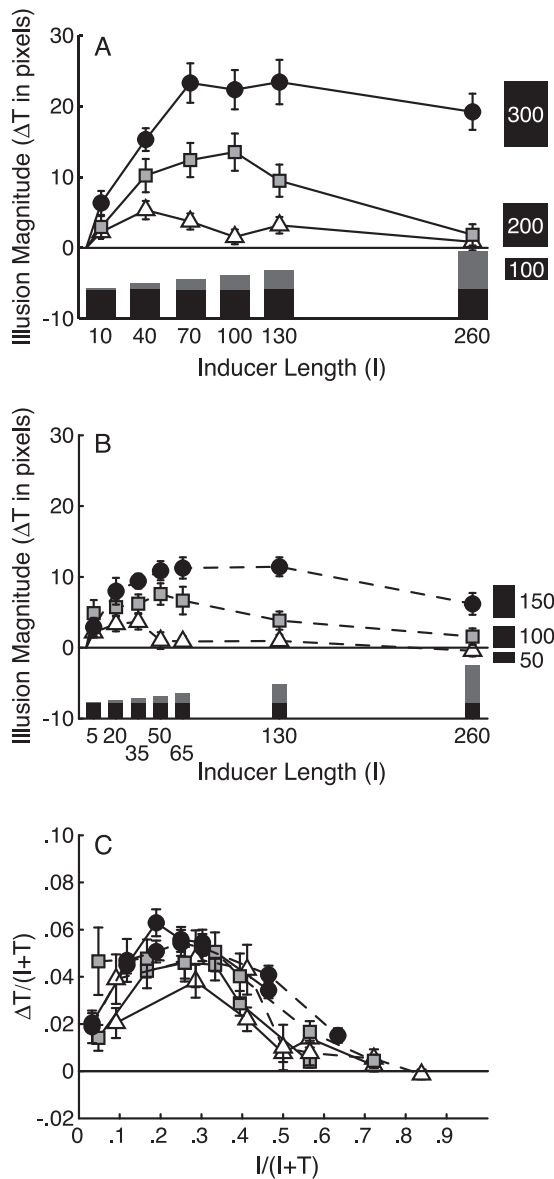


Figure 5. CSI magnitude (ΔT) as a function of inducer extent (I) and target extent (T) for the large configurations (A) and small configurations (B) and for CSI magnitude relative to the total extent [$(\Delta T / (I + T))$] as a function of inducer extent relative to the total extent [$I / (I + T)$] for the large and small configurations (C). Error bars represent the standard errors of the means.

the side than on the top of the target but only for the longest target, $F(2, 22) = 6.07$, $p < 0.01$ (i.e., when the target was 300 pixels tall by 100 pixels wide and the inducer was on top and when it was 100 pixels tall by 300 pixels wide and the inducer was on the side). The reason for this interaction is unclear. Note that we did not find effects of inducer location in Experiments 2 or 3, but those targets were square as in the present 200-pixel condition rather than elongated as in the present 300-pixel condition. As seen in Figure 5A, the effect of target extent is monotonic over the tested range; linear contrast, $F(1, 11) = 96.72$, $p < 0.001$. As in Experiment

3, the effect of inducer extent is nonmonotonic, peaking at midsize inducers, with a robust quadratic contrast, $F(1, 11) = 43.02$, $p < 0.001$, and a weaker linear contrast, $F(1, 11) = 5.87$, $p < 0.05$. There was also an interaction between target and inducer extent, $F(10, 110) = 10.94$, $p < 0.001$, due to the size of the illusion peaking at longer inducer extents for longer targets. The maximal CSI occurs when the inducer is roughly 25% to 30% of the total configural extent ($I + T$).

The results for the small-configuration condition (Figure 5B) were similar to those for the large-target condition (Figure 5A) except that the illusion was approximately half as large. There were main effects of target length, $F(2, 30) = 15.43$, $p < 0.001$, and inducer length, $F(6, 90) = 9.75$, $p < 0.001$. There was also a similar interaction between target size and inducer location as for the large configurations, $F(2, 30) = 5.68$, $p < 0.01$, but the reason is still unclear. The effect of target was monotonic [linear contrast: $F(1, 15) = 39.91$, $p < 0.001$] and the effect of inducer extent was nonmonotonic [quadratic contrast: $F(1, 15) = 49.41$, $p < 0.001$; linear contrast: $F < 1$], peaking at midsize inducers. There was also a similar inducer \times target-length interaction in which the illusion peaked at longer inducers for longer targets, $F(2, 30) = 6.15$, $p < 0.001$. For these smaller configurations, the maximal CSI occurs when the inducer is roughly 30% of the total configural extent ($I + T$).

Figure 5C shows the data from Figure 5A and B replotted to show the approximate invariance of the CSI when scaled relative to the extent of the whole configuration ($I + T$). (Note that some variation in Figure 5C may result from having different participants in the large- and small-configuration conditions.) The y-axis represents the ratio of illusion magnitude from Figure 5A and B (ΔT , where T is the target extent in pixels and ΔT is the increase due to the CSI to the extent of the total configuration ($I + T$, where I is the extent of the inducer in pixels)). This transformation largely removes the difference between larger and smaller configurations and the effects of the different target sizes evident in Figure 5A and B. The x-axis represents the extent of the inducer (I) relative to the total configuration ($I + T$). This transformation brings the peaks of the inducer extent functions into approximate alignment, with a maximum illusion of 6% of the configural extent when the inducer composes 20% to 30% of the entire configuration. The only systematic effect apparent in Figure 5C is that of inducer extent relative to the whole configuration, $I / (I + T)$. This fact implies that the illusion is primarily driven by this factor and that, if the shape of this inverted-U function can be explained, the rest of the data in Figure 5A and B can be predicted simply by scaling the relative extent variables in Figure 5C back into absolute stimulus extents.

We next conducted a multiple linear regression analysis on the untransformed data to better understand the interaction between target and inducer length on the CSI and to confirm that the absolute size of the target does not contribute significantly to the illusion magnitude when considered separately from the size of the inducer. We predicted the CSI magnitude for the large (Figure 5A) and small (Figure 5B) configurations from the following two factors: the logarithm of inducer length (given the shape of the curves in Figure 5) and inducer length relative to the length of the whole configuration, $I/(I + T)$. The best-fitting model was

$$CSI' = -5.3 + 11.7 * \log(I + 1) - 75.4 * \frac{1}{I + T}, \quad (1)$$

which explained 71% of the variance. The extent of the target did not account for additional variance beyond that explained by these two factors.

Experiment 5

The results of Experiment 4 established that CSI magnitude depends on the relative extents of both the target and inducer. This finding led us to ask whether the effect of the inducer is globally determined for the target within the configuration or whether its influence is local to the target edges shared with the inducer(s). In the global conception, the visual system's overall estimate of the target's length is influenced (and compromised) by a separate estimate of the extent of the whole configuration of which it is part. This is perhaps the simplest interpretation of Equation 1. Importantly, this model predicts that the magnitude of the illusion depends only on the size of the target relative to the size of the whole configuration.

There is an alternative interpretation, however, based on the mislocalization of specific edges. It assumes that the visual system makes its estimate of the extent of the target from the positions of edges that are seen as displaced toward the corresponding edges of the inducer. We tested this possibility experimentally by comparing two conditions: one in which the overall extent of the inducer was distributed entirely on one side of the target (e.g., all 80 pixels above the target, as in Experiments 1 through 4) and another in which the overall extent of the inducer was split equally between two sides of the target (e.g., 40 pixels above and 40 pixels below). If the effect of the inducer depends only on its total extent, then there should be no difference between the single-sided and double-sided inducer configurations in CSI magnitude. If mislocalization of the target's edges is the driving factor, however, the effect of two smaller inducers will be greater than that of one larger inducer, stretching the

perception of the target in opposite directions by acting on its two opposite edges.

Methods

Participants

All 23 participants had normal or corrected-to-normal vision and participated for partial course credit.

Design, displays, and procedure

The viewing conditions and equipment were the same as in the previous experiments. The displays consisted of the target on the left of the display (alone or with an inducer), and the adjustable rectangle was on the right. The target was always a square (100×100 pixels, the same as in the smaller stimulus condition of Experiment 4) and black (0.3 cd/m^2), the background was gray (50 cd/m^2), and the inducers were a darker gray (19 cd/m^2).

There were two single-inducer conditions (above or below the target) and one double-inducer condition (above or below the target). The width of all inducers was 100 pixels, and they were always aligned with the target. These three inducer location conditions were crossed with six inducer heights, producing 18 target/inducer configurations. In the single-inducer conditions the heights were 10, 20, 40, 80, 160, and 320 pixels. In the double-inducer condition the height of each inducer was half of that used in the corresponding single-inducer condition: 5, 10, 20, 40, 80, and 160 pixels. In the double-inducer condition the heights of the inducers above and below the target were always the same. Thus, the total size of the inducers present matched across the two conditions. There was also a no-inducer control condition, making a total of 19 target/inducer conditions.

For each configuration the adjustable rectangle was shown at two initial sizes: either wider or shorter than the target square ($125 \text{ pixels wide} \times 75 \text{ pixels high}$ plus a random number from -10 to $+10$ added to each dimension) or thinner or taller than the target square ($75 \text{ pixels wide} \times 125 \text{ pixels high}$ plus a random number from -10 to $+10$ added to each dimension). As in Experiments 1 and 4, the target configuration and comparison rectangle were positioned in a diagonal arrangement to prevent participants from using cues of alignment to aid their adjustments. In contrast with the previous experiments in which the comparison rectangle was in the bottom right corner of the monitor, the comparison rectangle was located 400 pixels above the target for half of the trials and 400 pixels below the target for the other half. This manipulation controlled for any influence that the relative vertical positions of the adjusted and target rectangles might have on the

size of the illusion. When the adjustable rectangle was in the bottom right of the monitor, the adjustment was the same as in Experiment 4, in which participants had control over the top left corner of the rectangle by moving the mouse. When the adjustable rectangle was in the top right of the monitor, participants had control over the bottom left corner of the rectangle. The two positions for the adjustable comparison rectangle were tested in separate blocks (counterbalanced over participants), and participants completed one practice trial before each block. There were 152 trials (19 target/inducer configurations including the control condition, two adjustable rectangle positions, two starting sizes of the adjustable rectangle, and two replications).

Results and discussion

The CSI magnitude was measured in the same way as in Experiments 1 and 4. We subtracted the adjusted height and width of the adjusted rectangle in the no-inducer control condition from the height and width of the adjusted rectangle in each experimental condition (matched for each participant for each initial size in each replication for each adjustable rectangle location). We expressed these differences as percentages of the target size (100 pixels). We first conducted a repeated-measures ANOVA to test whether the location for the single-sided inducer (above vs. below the target) affected the illusion magnitude in the height dimension. As in Experiment 3, inducer location had no effect ($F < 1$). We therefore averaged over the two single-sided inducer conditions for the remainder of the analyses and in Figure 6. We next conducted a four-way repeated-measures ANOVA on the illusion magnitude in the height dimension: 2 inducer types (single sided or double sided) \times 5 inducer lengths (see Methods) \times 2 adjustable rectangle locations (below-right or below-left of the target) \times 2 adjustable rectangle initial sizes (smaller or larger than the target). There was no main effect of the adjustable rectangle's location and it did not interact with the size of the inducers ($F < 1$), but there was a small interaction between the relative location of the adjustable rectangle and the number of inducers, $F(1, 22) = 5.66$, $p = 0.03$. When there was a single inducer, the illusion was 0.6 pixel larger when the adjustable rectangle was higher in the display, whereas when there were two inducers (the double-inducer condition) the illusion was 0.7 pixel larger when the adjustable rectangle was lower in the display. It is unclear why this effect occurred, and it did not influence the pattern in the effects of inducer size for the single- and double-inducer conditions ($F < 1$).

Average illusion magnitudes in the height dimension (averaged over participants, initial size, inducer position, and position of the adjustable rectangle) are

plotted in Figure 6A for the single- and double-sided targets relative to the total length of the inducer. In this plot, the y-values at a given x-value represent conditions in which the total length of the inducer(s) is the same, but it is either all on one side of the target or split between two sides. The curves reveal the same inverted-U shape as a function of inducer height as was evident in Experiments 3 and 4, with a main effect of inducer size, $F(5, 110) = 25.59$, $p < 0.001$, a significant quadratic trend, $F(1, 22) = 90.98$, $p < 0.001$, and no linear trend, $F(1, 22) = 1.66$, $p > 0.05$. There was also a main effect of number of inducers in which the illusion was greater overall for the double-inducer conditions than the single-inducer conditions with the same total inducer length, $F(1, 22) = 46.34$, $p < 0.001$. However, the number of inducers interacted with the total inducer length, $F(5, 110) = 12.89$, $p < 0.001$, as evident by the shift in the maximum, which occurred when the total inducer extent was 40 pixels in the single-inducer condition and 80 pixels in the double-inducer condition. This simply means that the maximum occurred in both the single- and double-inducer functions when the individual inducers were 40 pixels long, as shown in Figure 6B. For the three middle inducer lengths tested, the magnitude of the illusion is consistently about 1.5 times larger in the double-inducer condition than in the corresponding single-inducer condition.

Collectively, these results support the local edge-based mislocalization theory. First, when total configuration size is compared in Figure 6A, having two smaller inducers on either side leads to a larger illusion than does having one larger inducer. Second, the degree to which inducer extent influences the magnitude of the illusion shows a consistent pattern when expressed in terms of the number of single-sided inducers present (one or two) and the extent of those inducers (from 10 to 160 pixels), as shown in Figure 6B. The maximum influence of the inducers occurred when each inducer was 40% as tall as the target, regardless of the number of inducers present, and the illusion magnitude in the double-sided conditions was approximately constant (1.5 times larger than in the single-inducer conditions) when expressed as a function of the inducer extent along one edge of the target. This shows that the inducer on each side has an incremental effect on the perceived shape of the target, as expected from an edge-based mislocalization explanation.

General discussion

We have reported evidence of a new illusion in which observers perceive a target region of a well-defined shape to be selectively elongated in a direction consistent with the extent of the larger configuration of which it is part.

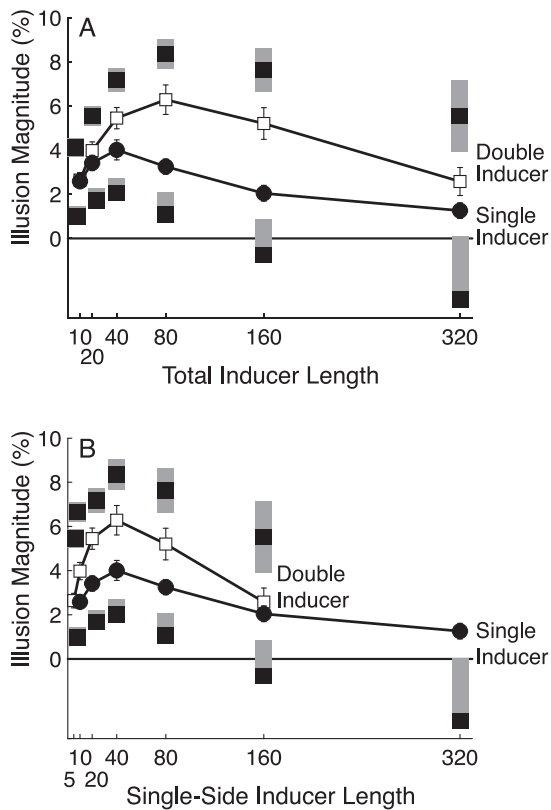


Figure 6. CSI magnitude as a function of total inducer length for the single-inducer condition (black circles) and the double-inducer condition (white squares) (A) and as a function of the single-sided inducer length (B). Errors bars represent the standard errors of the means.

The results of Experiments 1 through 3 show that the magnitude of this illusion is invariant over (a) the position of the inducer relative to the target (above, below, left, or right), (b) the relative perceived depth or occlusion of the target and inducer, and (c) the polarities of lightness contrast among target, inducer, and background. The illusion's magnitude varies systematically with several factors that are known to influence the strength of perceptual grouping between the target and inducer: proximity, alignment (good continuation), lightness similarity, hue similarity, and common fate (Wagemans et al., 2012; Wertheimer, 1923, 2012). We call the illusion the Configural Shape Illusion (CSI) because of these grouping-related effects, which influence the perceived shape of the target to the extent that the target and inducer form a unified configuration.

The results of Experiments 3 and 4 demonstrate that CSI magnitude is strongly influenced by the relative extents of the inducer and target. In particular, CSI magnitude follows an inverted U-shaped function over inducer extent, where the illusion increases as the inducer length increases to a critical length ($\sim 30\%$ the whole configuration) and then decreases. The shape of this curve is largely invariant when illusion magnitude

is plotted as a proportion of the extent of the whole configuration, $\Delta T/(I+T)$, as a function of the extent of the inducer relative to the extent of the whole configuration, $I/(I+T)$ (Figure 5C).

The results of Experiment 5 show that two-sided inducers produced robustly larger illusions than did corresponding one-sided inducers of the same total extent. For example, two 40-pixel-long inducers on opposite edges of the target produced a much larger effect than did a single 80-pixel-long inducer on just one edge. This finding implies that the illusion is based on mislocalization of edges (e.g., Morgan, Hole, & Glennerster, 1990) rather than on misestimated lengths, or “framing ratios” of the target's length, relative to the whole configuration (e.g., Brigell et al., 1977). The combined effect of two-sided inducers fell short of being fully additive, however, as the illusion magnitude of a two-sided inducer was only about 1.5 times greater (rather than twice as great) than that of a one-sided inducer of the same extent.

The inverted U-shaped function over inducer extent that is present in the CSI (Experiments 3 through 5) has also been shown to occur in several classic illusions of extent, including the Müller-Lyer, Baldwin, Divided Line, Parallel Lines, and Brentano illusions (e.g., Brigell, Uhlarik, & Goldhorn, 1977; Bulatov, Bertulis, Bulatova, & Loginovich, 2009; Bulatov, Bertulis, Gutasukas, Mickiene, & Kadziene, 2010; Pressey, 1988; Pressey & Murray, 1976; Schiano, 1986). There are further commonalities between the CSI and some of these classic illusions. First, the Müller-Lyer illusion is modulated by grouping related factors, such as the color similarity and proximity relations between the wings and shaft (Brigell et al., 1977; Coren & Girgus, 1972), much in the same way that we have found for the CSI. Second, the Baldwin illusion scales with the overall size of the configuration (Brigell et al., 1977), as we found for the CSI in Experiment 4. Such similarities suggest that these illusions might share the same or similar underlying mechanism, as we discuss below.

The primary questions of interest are why the CSI occurs and whether the mechanisms responsible for it are related to the mechanisms underlying the other illusions mentioned. The evidence reported above is most consistent with an edge-based assimilation account, in which the positions of the target's actual borders appear to be assimilated toward the corresponding borders of the whole configuration. The degree of assimilation is partly determined by the degree to which the target and inducer are related by virtue having similar perceptual features or by virtue of being grouped into a single configuration. It is not yet clear whether grouping is actually a mediating factor in the CSI or whether mere similarity in terms of grouping variables is sufficient. An account based solely on grouping or similarity cannot, however, account for the

inverted U-shaped function over inducer extent. Grouping by shape or size similarity should be strongest when the inducer is 50% of the length of the whole configuration, yet the maximal illusion occurs when the inducer is only about 30% of the length of the whole configuration.

A plausible explanation can be derived by considering edge assimilation effects that result from spatial pooling across overlapping receptive fields (RFs) that may contain an irrelevant inducer edge as well as the relevant target edge (e.g., Morgan et al., 1990). This type of edge-based spatial averaging model, which we further describe below, has previously been applied to account for illusions of extent for a line or a space flanked by contextual objects (e.g., Bulatov et al., 2009; Bulatov et al., 2010; Morgan et al., 1990) and errors in the perceived location of dots (e.g., Prinzmetal, 2005). Other assimilation models have been based on misestimation of length (Brigell et al., 1977; Jaeger & Long, 2009) and spatial averaging with attentional fields (e.g., Pressey, 1988; Pressey & Murray, 1976). Given that the CSI depends on the number of inducers and not just the extent of the global configuration (see Experiment 5), the CSI is better explained by models based on mislocalized edges than by those based on misestimated length. Because we did not manipulate attention in the present experiments, the present data are silent about whether the RF pooling described below is based purely on low-level sensory information or is modulated by attention.

Our own account of the CSI is similar to these assimilation models in its first three assumptions, but adds a fourth assumption to explain the grouping or similarity effects of Experiments 1 and 2. We suggest that the results of the five experiments reported above can be explained by the following four assumptions.

(1) **Distributed population coding of edge position.** The position of an edge is coded as the maximum of the population of a positionally distributed set of units that respond to the target edge within their spatially limited RFs. When the target edge is the only edge present within the RFs responding to that target edge, its position will be accurately encoded in the population response of those units. This implies that perception of target extent will be accurate under two conditions: when only target edges have been presented (in a control condition, in which the inducer extent is zero) and when inducer edges are so far from target edges that the former lie outside the RFs of all units that respond to the latter. Accordingly, the CSI should eventually reach zero when the inducer's outer edge is far enough away or when the entire inducer is separated from the target by a large enough gap. Errors that do occur will be normally distributed with no resulting bias in the mean perceived location (Prinzmetal, 2005).

(2) **Probability of multiple edges falling within the same RF.** We assume that the probability that an inducer edge falls within the RF of a unit that responds to the target edge decreases monotonically as the distance between the target and inducer edges increase. That is, as the outer inducer edge is positioned farther from the target edge, the influence of the inducer diminishes because it affects fewer units in common with the target edge.

The presence of the inducer edge will therefore increase the responses of RF units whose centers lie in the direction of the inducer edge, thus shifting the maximum in the population response toward a position between the target edge and the inducer edge. It follows that, as the distance from the target edge to the inducer edge increases, the maximum in the population response to the target edge will increase monotonically for RFs that include both edges. This relation largely explains the rapid increase in the size of the illusion as the distance of the inducer edge increases to about 30% of the total configuration length. Assumption 2 operates over the entire range of inducer extents studied above. The precise nature of the decrease in probability with distance will therefore determine the shape of the curve expressing illusion magnitude as a function of inducer extent, at least when both are expressed as proportions of the total configural extent (Figure 5C). The net decrease in illusion size when the inducer is more than about 30% of the whole configuration is primarily attributed to this assumption, which is based on spatially limited RF sizes.

(3) **Proportional coding of configurations.** The RF sizes that code the positions of the target and inducer edges increase with the size of the total configuration (i.e., larger configurations are coded in terms of proportionally larger RFs). This assumption corresponds to the scale-invariance finding in Experiment 4 that CSI magnitude is more parsimoniously expressed as a relative function of configural size ($I + T$) than as an absolute function of the distance between the target and inducer edges (I).

(4) **Weighted summation of RF responses to multiple edges.** We assume that when the outer inducer edge falls within the RF of the same units that responds to the target edge, the output of that unit will increase to a degree that depends on a weight reflecting the similarity of that edge to the target's edge (i.e., higher similarity produces greater net output) or the degree to which the edges are grouped within a single configuration. Importantly, assumption 4 reflects the differential weighting that occurs when the target and inducer shapes are more (or less) similar or closely related in relevant ways. Accordingly, the amount of edge mislocalization is reduced to the degree that the target and inducer are

differentiable as separate objects having distinct properties. When the target and inducer are similar in lightness, proximity, good continuation, hue, and common fate, the visual system faces a greater challenge of isolating the target's edge from the edge of the global configuration. This assumption can also account for why target–inducer grouping by color similarity and proximity modulates the Müller-Lyer illusion (Coren & Girgus, 1972).

We note that the majority of the effects we initially attributed to grouping can be equally well explained as arising simply from similarity effects according to assumption 4. That is, as the inducer and target edges become more similar, the inducer causes a greater increment in the output of the units responding to the target edge and thus a greater shift in the maximum of the population response coding the target edge's position. We view it as an open question whether such similarity effects are equivalent to grouping effects or whether grouping implies some additional processing mechanism, such as attention. This possibility may be relevant to determining whether the CSI is due purely to low-level RFs or to higher-level attentive fields (e.g., Pressey, 1971, 1988).

The foregoing assimilation account of the CSI implies the existence of further effects that should be examined experimentally. One clear implication is that there should be CSI-like illusions of extent in the *negative* direction (i.e., making the target appear *smaller*) when the target's edges are *inside* the inducer's edges. Indeed, there is evidence for this effect in the results of Experiment 1. When the inducer was located inside the target (see Figure 1B, right side), a negative illusion in which the target appeared to be smaller than it actually was in both vertical and horizontal directions was evident rather than producing no illusion, as originally expected. Such negative illusions are inherent in length-reducing portions of classic illusions of extent (e.g., the wings-in version of the Müller-Lyer illusion).

In a similar vein, an edge-based assimilation effect of the type we propose for the CSI may be responsible for the “shrinkage illusion” of Kanizsa and Luccio (1978) (see Figure 7). The illusion is that when the central portion of a target (here, a white rectangle) is partly covered by an inducer (here, a black rectangle), the partly occluded target appears to be shorter (and perhaps wider) than the physically identical figure without an inducing occluder. The explanation in terms of edge-based assimilation would be that the sides of the white target rectangle appear to be displaced toward the nearby parallel edges of the black inducer rectangle, thereby causing the larger white target to appear shorter than the physically equivalent figure [Palmer & Schloss, in press; see also Vezzani (1999) for mention of Luccio's (1981) assimilation account].

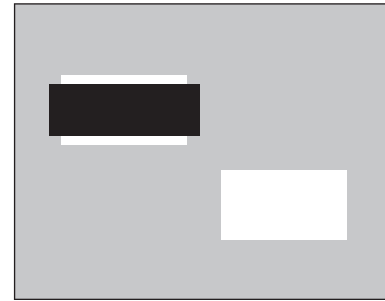


Figure 7. A version of the shrinkage illusion (Kanizsa & Luccio, 1978). The partly occluded white target figure appears shorter than the physically identical white rectangle without the black inducer.

Another implication of the present account of the CSI is that the same mechanisms should produce illusions of increased (or decreased) overall size if the target lies wholly inside (or wholly outside) an inducer that is a correspondingly enlarged (or reduced) version of the same shape. If true, the well-known Delboeuf size illusion is also related to the CSI in that the target figure is enlarged or reduced uniformly in both directions rather than selectively in one dimension. These and other implications of the edge-based assimilation account of the CSI discussed above naturally require further study, but they deserve to be investigated more fully, both empirically and theoretically.

Keywords: perceptual organization, assimilation, population coding

Acknowledgments

We thank James Pomerantz and an anonymous reviewer for their helpful comments on this manuscript. We also thank Bill Prinzmetal, Marty Banks, Joseph Austerweil, Eli Strauss, and Lily Lin for their help with this study. The project was supported by the National Science Foundation (BCS-1059088 and BCS-0745820).

Commercial relationships: none.

Corresponding author: Karen B. Schloss.

Email: karenschloss@gmail.com.

Address: Department of Cognitive, Linguistic, and Psychological Science, Brown University, Providence, RI, USA.

Footnote

¹The percentage of the monitor is calculated for an object as its length in pixels in a given dimension (width

or height) divided by the length of the monitor (1680 pixels wide \times 1050 pixels high) in that dimension. This calculation can be done to characterize all the stimuli with respect to the size of the monitor. In analyzing the data we did not specifically discount the size and dimensions of the monitor's screen, but to the extent that their effects are also present in the no-inducer control condition, subtraction of the no-inducer results from those of the other conditions (see the Results and discussion section) eliminates such effects from the CSI magnitudes reported in this article.

References

- Avery, G., & Day, R. (1969). Basis of the horizontal-vertical illusion. *Journal of Experimental Psychology*, *81*(2), 376–380.
- Brigell, M., Uhlarik, J., & Goldhorn, P. (1977). Contextual influences on judgments of linear extent. *Journal of Experimental Psychology: Human Perception and Performance*, *3*(1), 105–118.
- Bulatov, A., Bertulis, A., Bulatova, N., & Loginovich, Y. (2009). Centroid extraction and illusions of extent with different contextual flanks. *Acta Neurobiologiae Experimentalis*, *69*, 504–525.
- Bulatov, A., Bertulis, A., Gutasukas, A., Mickiene, L., & Kadziene, G. (2010). Center-of-mass alterations and visual illusion of extent. *Biological Cybernetics*, *102*, 475–487.
- Coren, S., & Girgus, J. S. (1972). Differentiation and decrement in the Mueller-Lyer illusion. *Perception and Psychophysics*, *12*(6), 466–470.
- Finger, F. W., & Spelt, D. K. (1947). The illustration of the horizontal-vertical illusion. *Journal of Experimental Psychology*, *37*, 243–250.
- Jaeger, T., & Long, S. (2009). Classical illusions from parallel line figures: Evidence for interactions among length-coding neurons. *Perceptual and Motor Skills*, *109*(2), 452–458.
- Kanizsa, G. (1979). *Organization in vision: Essays on Gestalt perception*. New York: Praeger.
- Kanizsa, G., & Luccio, R. (1978). *Espansione di superficie da completamento amodale. Reports from the Institute of Psychology, University of Trieste, Trieste, Italy*.
- Luccio, R. (1981). Effetti dimensionali del completamento amodale: Un'analisi in termini di assimilazione. *Giornale Italiano di Psicologia*, *8*, 375–392.
- Morgan, M. J., Hole, G. J., & Glennerster, A. (1990). Biases and sensitivities in geometrical illusions. *Vision Research*, *30*(11), 1793–1810.
- Palmer, S. E. (1999). *Vision science: Photons to phenomenology*. Cambridge, MA: MIT Press.
- Palmer, S. E., Brooks, J. L., & Lai, K. S. (2007). The occlusion illusion: Partial modal completion or apparent distance? *Perception*, *36*, 650–669.
- Palmer, S. E., & Rock, I. (1994). Rethinking perceptual organization: The role of uniform connectedness. *Psychonomic Bulletin and Review*, *1*(1), 29–55.
- Palmer, S. E., & Schloss, K. B. (2009). Stereoscopic depth and the occlusion illusion. *Attention, Perception, and Psychophysics*, *71*, 1083–1094.
- Palmer, S. E., & Schloss, K. B. (in press). The occlusion, configural shape, and shrinkage illusions. In D. Todorovic & A. G. Shapiro (Eds.), *Oxford compendium of visual illusions*. Oxford, UK: Oxford University Press.
- Pressey, A. W. (1971). An extension of assimilation theory to illusions of size, area, and direction. *Perception and Psychophysics*, *9*(2), 172–176.
- Pressey, A. W. (1988). In defense of the assimilation theory of visual illusions. *Perceptual and Motor Skills*, *66*, 760–762.
- Pressey, A. W., & Murray, R. (1976). Further developments in the assimilation theory of geometric illusions: The adjacency principle. *Perception and Psychophysics*, *19*(6), 536–544.
- Prinzmetal, W. (2005). Location perception: The X-Files parable. *Perception and Psychophysics*, *67*(1), 48–71.
- Schiano, D. J. (1986). Relative size and spatial separation: Effects on the parallel-lines illusion. *Perceptual and Motor Skills*, *63*, 1151–1155.
- Vezzani, S. (1999). Shrinkage and expansion by amodal completion: A critical review. *Perception*, *28*, 935–947.
- Wagemans, J., Elder, J. H., Kubovy, M., Palmer, S. E., Peterson, M. A., Singh, M., et al. (2012). A century of Gestalt psychology in visual perception: I. Perceptual grouping and figure-ground organization. *Psychological Bulletin*, *138*(6), 1172–1217.
- Wagner, G., & Boynton, R. M. (1972). Comparison of four methods of heterochromatic photometry. *Journal of the Optical Society of America*, *62*, 1508–1515.
- Wertheimer, M. (1923). Untersuchungen zur Lehre von der Gestalt. II. *Psychological Research*, *4*(1), 301–350.
- Wertheimer, M. (2012). Investigations on Gestalt principles (M. Wertheimer & K. W. Watkins, Trans.). In L. Spillman (Ed.), *On perceived motion and figural organization* (pp. 127–183). Cambridge, MA: MIT Press.